Supplementary Material for

Novel Mechanistic PBPK Model to Predict Renal Clearance in Varying Stages of CKD by Incorporating Tubular Adaptation and Dynamic Passive Reabsorption

Weize Huang and Nina Isoherranen

Department of Pharmaceutics, School of Pharmacy, University of Washington, Seattle, WA, 98195

Supplemental Methods for Development of the Adaptation Factors

The adaptive model incorporates the physiologically-based adaptation of tubular water reabsorption in CKD patients to parameterize tubular flow rate (TFR) of all model subsegments to allow the TFR to decrease less than proportionally in relation to GFR. As TFR for each subsegment is a model-specific parameter and depend on the number of kidney segments included in the model, the quantitative approach for the physiological adaptation is also only directly applicable for the specific previously developed mechanistic kidney model for healthy kidney[2] that has 11 longitudinal subsegments. To quantitatively describe the adaptation of tubular water reabsorption, a set of tubular subsegment-specific adaptation factors (AF_i) was calculated based on reported mean urine formation of 0.62 mL/min (62% of healthy urine flow) in CKD patients (n=216) with a mean GFR of 10 mL/min (8.3% of healthy GFR).[1] Physiologically and mathematically, the magnitude of adaptation of TFR in CKD patients must be different in different tubular subsegments and monotonically increase from proximal segment to collecting duct. The inflow of the first subsegment of the proximal tubule must equal GFR and as such must decline proportionally with GFR, indicating no adaptation in this subsegment. In contrast, the outflow of the last subsegment of the collecting duct cannot decline proportionally to GFR as this would result in a urine flow of 0.083 mL/min, a value that is 83% lower than the observed urine flow of 0.6 mL/min when GFR =10 mL/min. As such (*vide infra*), to match the observed urine flow in CKD patients, the collecting duct must have the maximum adaptation, and TFR in this subsegment must decline much less than GFR. To meet these requirements, the tubular subsegment-specific AF (AF_i) for each TFR was calculated using Equation 1:

$$Adaptation\ Factor_i\ (AF_i) = min + \frac{max - min}{1+10^{n(Log_{10}TFR_{i,H}-1)}} \qquad (1)$$

where min represents the minimum adaptation capacity of 0, max represents the maximum adaptation capacity of 0.57, n is analogous to Hill coefficient which was set at 1.80. $TFR_{i,H}$ represents the individual value of renal tubular flow rate entering each tubular subsegment (including bladder) in healthy subjects (i.e. GFR = 120 mL/min) where i ranges from 1 to 12 and H stands for healthy state. The values of tubular flow rates in healthy subjects are based on human physiology and as published previously.[2]

The mathematical structure of Equation 1 was chosen based on biological plausibility to adhere to mass balance principles of liquid flow in the kidney. Other functions such as linear, exponential, logarithmic, power, and Michaelis-Menten variant functions were also tested but all of these functions failed to produce a physiologically possible tubular flow profile for the 11 subsegment-based kidney model. All of these functions produced tubular flow rates for some subsegments that exceeded the value of the previous subsegment, a biologically impossible result due to conservation of matter (i.e. the TFR in downstream subsegment must be the same or lower than the previous subsegment) and hence could not be included. To maintain mass balance of liquid flows in the kidney, tubular flow rate must decrease monotonically from proximal segment to collecting duct as water is being reabsorbed. The water reabsorption in the model is incorporated as the difference in tubular flow rate between individual subsegments.

In equation 1 the parameter n (analogous to Hill coefficient) was set as 1.8 after optimization based on biological plausibility of monotonically decreasing tubular flow rate. Other tested values for n were not plausible; for example, if n = 1.6, when GFR = 5 mL/min, the second subsegment will have a tubular flow rate of 5.3 mL/min, which exceeds the GFR value of 5 mL/min. If n = 2, when GFR = 5 mL/min, the 6^{th} subsegment will have a tubular flow rate of

2.94 mL/min, but the 7th subsegment will have a tubular flow rate of 3.18 mL/min, exceeding the tubular flow rate of the previous subsegment.

Overall, Equation 1 generates a series of adaptation factors that are applied to each subsegment in our model to specifically address the quantitative changes in water reabsorption in the kidney with CKD. Since the adaptation factor is specific to the TFR in each model subsegment, equation 1 incorporates the TFR for a subsegment in the calculation. The model-specific adaptation factors are then incorporated with patient's GFR into Equation 2:

$$Scalar_{ij} = 1 - (1 - \frac{GFR_j}{120}) \times (1 - AF_i) \quad (2)$$

to calculate a scalar that is both segment-dependent and CKD stage/GFR-dependent.

Table S1. Representative tubular flow rates (TFR) for the proportional and adaptive models at different stages of CKD. The tubular subsegment-dependent adaptation factors (AF_i) were calculated according to Equation 1 and implemented for the adaptive model. The renal tubular flow rates (TFR) were calculated using either proportional model (TFR_P) by direct scaling to GFR as described in Methods, or using the adaptive model (TFR_A) according to Equations 2 and 3. The renal tubular flow rate (TFR) (mL/min) shown here indicates the inflow rate of entering each renal subsegment, which equals to the outflow rate exiting from the previous renal subsegment. The inflow rate of the first proximal tubule subsegment always equals to the GFR. The outflow rate of the last subsegment of collecting duct always equals to the inflow rate of bladder and the urine formation rate (as no reabsorption occurs within bladder). All flows are presented in mL/min.

	Healthy (Stage 1) GFR = 120 mL/min		Mild Stage CKD (Stage 1/2) GFR = 90 mL/min		Moderate Stage CKD (Stage 2/3) GFR = 60 mL/min		Severe Stage CKD (Stage 3/4) GFR = 30 mL/min		End Stage CKD (Stage 4/5) GFR = 15 mL/min	
Model Subsegment	TFR	Adaptation Factor	TFR_P	TFR_A	TFR_P	TFR_A	TFR_P	TFR_A	TFR_P	TFR_A
$Proximal\ Tubule_1$	120	0	90.00	90.00	60.00	60.00	30.00	30.00	15.00	15.00
$Proximal\ Tubule_2$	94	0.0099	70.50	70.73	47.00	47.47	23.50	24.20	11.75	12.57
$Proximal\ Tubule_3$	68	0.018	51.00	51.30	34.00	34.60	17.00	17.89	8.50	9.54
$Loop\ of\ Henle_D$	43	0.038	32.25	32.66	21.50	22.33	10.75	11.99	5.38	6.82
$Loop\ of\ Henle_A$	24	0.098	18.00	18.59	12.00	13.17	6.00	7.76	3.00	5.05
Distal Tubule	24	0.098	18.00	18.59	12.00	13.17	6.00	7.76	3.00	5.05
$Collecting\ Duct_1$	11	0.26	8.25	8.97	5.50	6.93	2.75	4.90	1.38	3.88
$Collecting\ Duct_2$	9	0.31	6.75	7.45	4.50	5.90	2.25	4.36	1.13	3.58
$Collecting\ Duct_3$	7	0.37	5.25	5.90	3.50	4.81	1.75	3.71	0.88	3.16
$Collecting\ Duct_4$	5	0.44	3.75	4.30	2.50	3.61	1.25	2.91	0.63	2.56
$Collecting\ Duct_5$	3	0.51	2.25	2.63	1.50	2.27	0.75	1.90	0.38	1.72
Bladder (Urine)	1	0.56	0.75	0.89	0.50	0.78	0.25	0.67	0.13	0.62

Table S2. Summary of the physicochemical and pharmacokinetic properties for the 20 test compounds used for adaptive model verification and comparison of the simulated and observed renal clearances for all test compounds used for model verification (Figures 3, 4, 5, and 6).

Drug	pK_a (acid)[a]	pK_a (base)[a]	$f_{u,p}$	Permeability (10^{-6} cm/s)	Observed Mean CL_r in Healthy (mL/min)	Simulated Mean CL_r in Healthy (mL/min)	Sim/Obs Ratio of CL_r in Healthy	Observed Mean CL_r in CKD4/5 (mL/min)	Simulated Mean CL_r in CKD4/5 (mL/min)	Sim/Obs Ratio of CL_r in CKD4/5
Parent-Metabolite Test Compounds in Figure 3										
Rotigotine	-	10.97	0.11[3]	19.5[4]	3.7[3]	4.8	1.30	1.8[3]	1.9	1.03
Acetaminophen	-	-	0.8[5]	35[6]	13[7]	15	1.15	7.1[7]	5.5	0.78
Lamotrigine	-	5.87	0.44[5]	88[6]	3.4[8]	3.1	0.92	1.9[8]	2.1	1.13
Rotigotine Glucuronide	-	-	1[b]	0.1[b]	110[3]	119	1.08	27[3]	22	0.82
Acetaminophen Glucuronide	-	-	1[b]	0.1[b]	108[7]	119	1.10	17[7]	15	0.88
Lamotrigine Glucuronide	-	-	1[b]	0.1[b]	114[8]	119	1.04	13[8]	18	1.37
Nonpermeable Test Compounds in Figure 4										
Melagatran	3.2	11.5	0.93[9]	0.145[9]	94[10]	110	1.17	12[10]	12	0.97
Sotalol	-	9.43	0.83[11]	0.26[12]	107[13]	99	0.92	19[13]	16	0.81
Gabapentin	4.63	9.91	0.97[9]	0.67[9]	99[14]	110	1.12	12[14]	16	1.30
Nadolol	-	9.76	0.8[11]	1.4[6]	82[15]	94	1.15	8.0[16]	8.0	1.00
Ribavirin	-	-	1[9]	1.55[9]	107[17]	106	0.99	10[17]	18	1.76
Doxycycline	3.27	8.33	0.1[11]	1.8[18]	15[19]	10	0.71	2.0[19]	2.0	0.98
Permeable Test Compounds in Figure 5										
Pefloxacin	5.66	6.47	0.75[9]	63.7[9]	7.5[20]	6.4	0.86	2.9[21]	3.1	1.05
Metronidazole	-	-	0.89[22]	64.7[9]	6.8[23]	7.3	1.08	2.6[23]	4.4	1.73
Minocycline	2.9	7.9	0.24[24]	76[25]	1.5[26]	1.1	0.70	0.98[26]	0.85	0.87
Digitoxin	7.18	-	0.05[27]	30[c]	0.85[27]	1.2	1.37	0.62[27]	0.38	0.62
Cicletanine	-	-	0.07[28]	95[c]	0.42[28]	0.36	0.86	0.19[28]	0.29	1.52
Pirfenidone	-	-	0.42[29]	120[c]	1.7[29]	1.7	0.99	0.96[29]	1.5	1.53
Secreted Test Compounds in Figure 6										
Para-aminohippuric Acid (PAH)	3.83	4.24	1	0.72[30]	599[31]	500	0.84	76[32]	86	1.12
Memantine	-	10.7	0.55[33]	25[34]	70[35]	77	1.10	16[35]	17	1.10

[a]pK_a values are obtained from https://www.drugbank.ca/
[b]experimentally determined metabolite data are not available, therefore these values are assumed based on physicochemical properties.
[c]experimentally determined data are not available, therefore permeability values were optimized using previously published and verified mechanistic kidney model with reported $f_{u,p}$ and observed CL_r in healthy subjects.

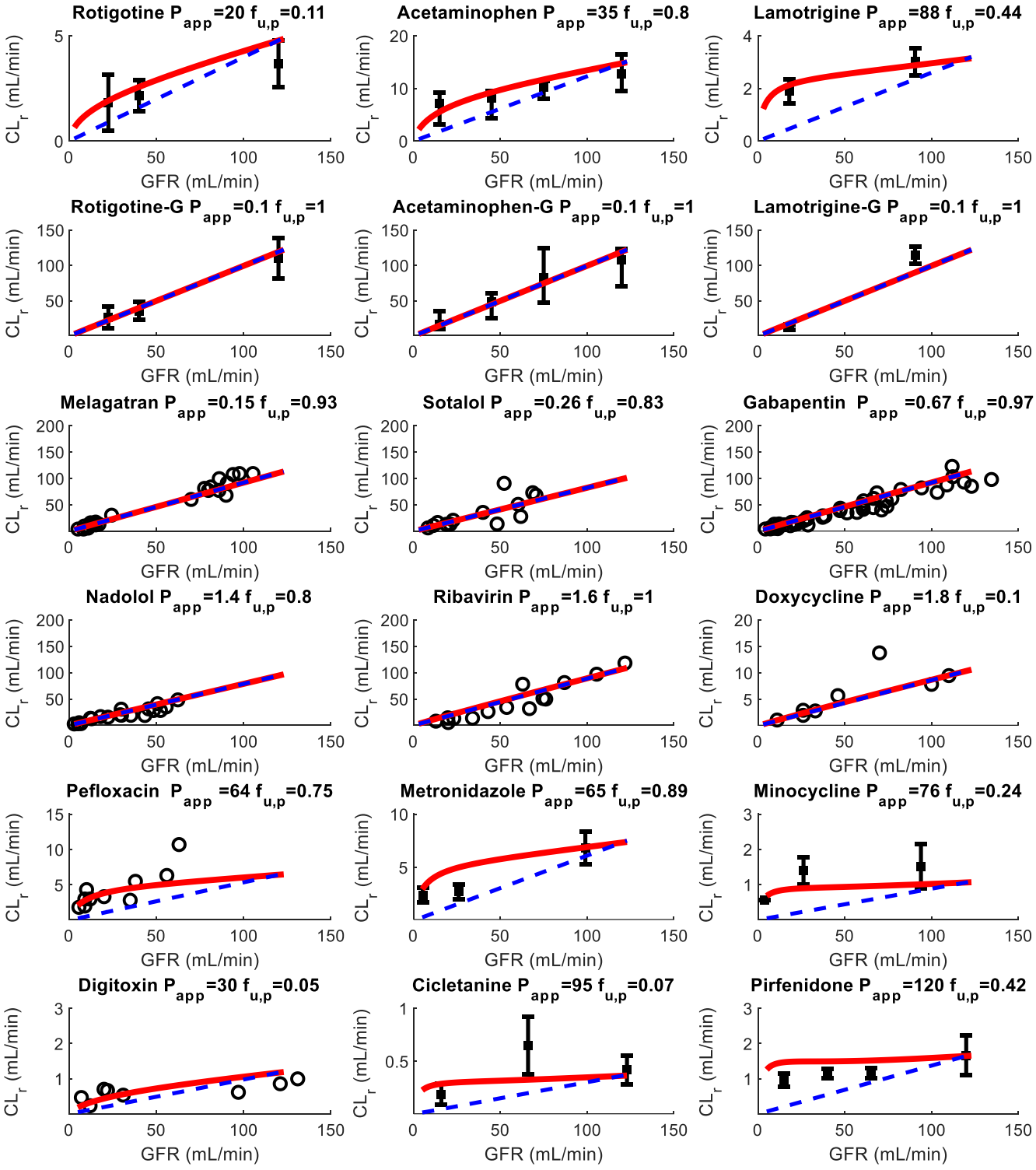

Figure S1. Linear plot of simulated versus observed renal clearance throughout CKD stages for all test drugs used for model verification.

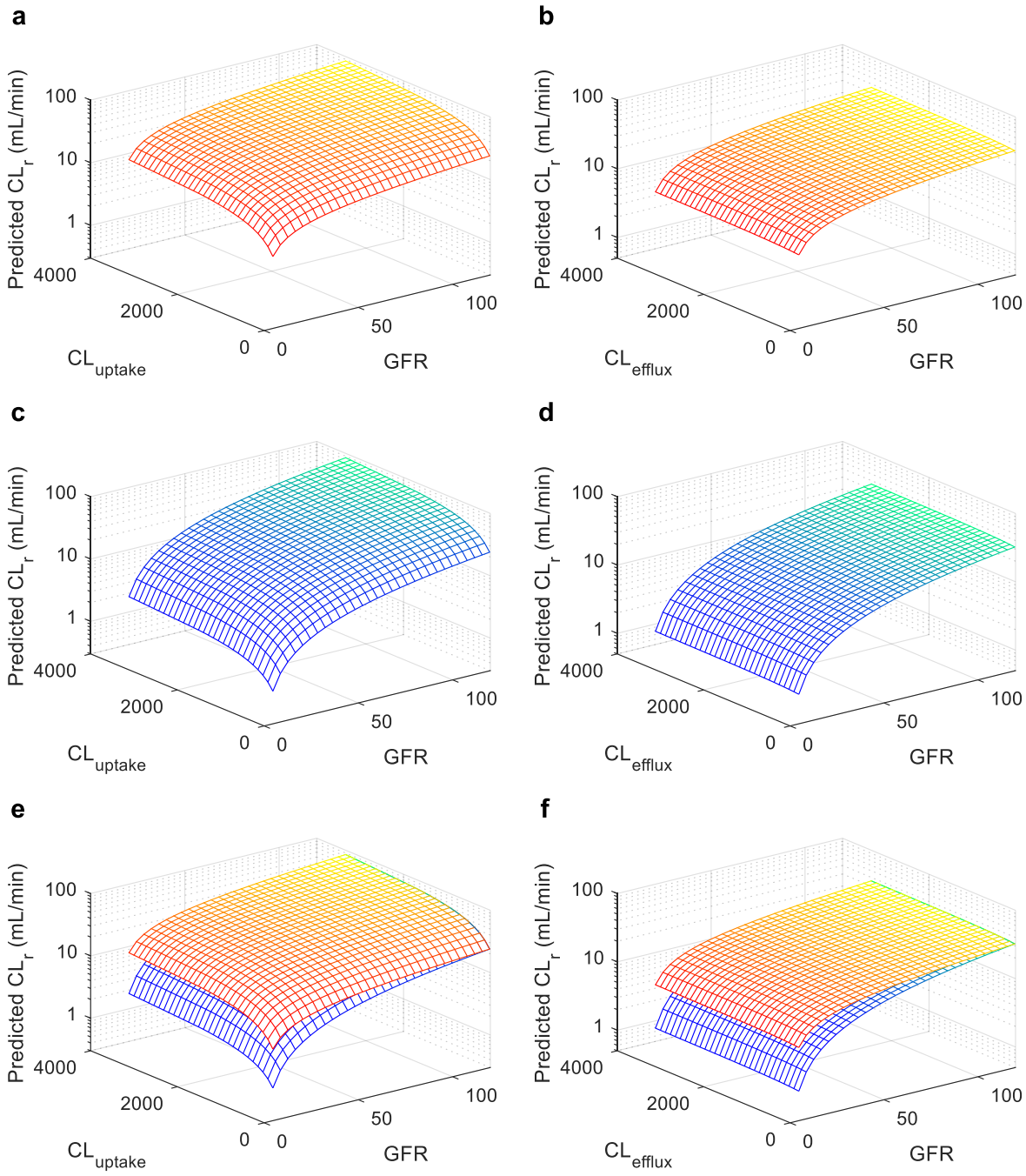

Figure S2. Sensitivity analyses of simulated renal clearance (CL_r in mL/min) at multiple stages of chronic kidney disease (CKD) reflected by varying glomerular filtration rates (GFR in mL/min) using adaptive model (shown in yellow-red) and proportional model (shown in blue-green). Left three panels (a,c,e) show the sensitivity analyses of simulated CL_r of neutral unbound permeable drugs ($f_{u,p}$ = 1, P_{app} = 30×10^{-6} cm/s) with a constant unbound intrinsic apical efflux transport clearance (CL_{efflux} = 150 mL/min) and different unbound intrinsic basolateral uptake transport clearances (CL_{uptake} = 10-3000 mL/min) across a range of GFRs (5-120 mL/min). Right three panels (b,d,f) show the sensitivity analyses of simulated CL_r of neutral unbound permeable drugs ($f_{u,p}$ = 1, P_{app} = 30×10^{-6} cm/s) with a constant unbound intrinsic basolateral uptake transport clearance (CL_{uptake} = 150 mL/min) and different unbound intrinsic apical efflux transport clearances (CL_{efflux} = 10-3000 mL/min) across a range of GFRs (5-120 mL/min).

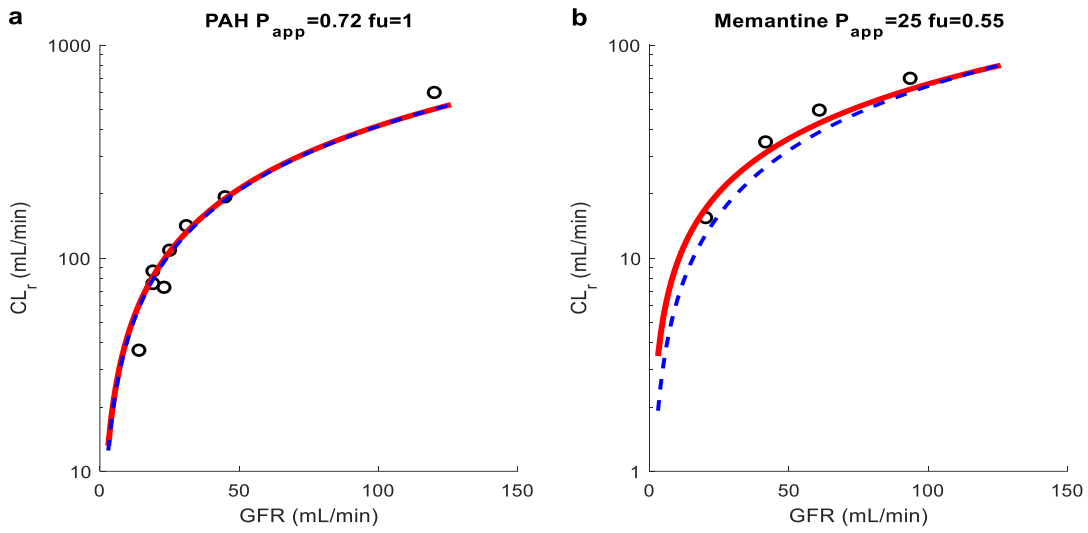

Figure S3. Simulations of CL_r of PAH and memantine using adaptive model (red) and proportional mode (blue) at multiple stages of chronic kidney diseases (CKD), and comparison to the observed individual data (PAH) and group mean data (memantine) shown in the black symbols.

References

1. Nechita, A. M. *et al.* Determining factors of diuresis in chronic kidney disease patients initiating hemodialysis. *J. Med. Life* **8**, 371–377 (2015).

2. Huang, W. & Isoherranen, N. Development of a Dynamic Physiologically Based Mechanistic Kidney Model to Predict Renal Clearance. *CPT Pharmacometrics Syst. Pharmacol.* **7**, 593–602 (2018).

3. Cawello, W., Ahrweiler, S., Sulowicz, W., Szymczakiewicz-Multanowska, A. & Braun, M. Single dose pharmacokinetics of the transdermal rotigotine patch in patients with impaired renal function. *Br. J. Clin. Pharmacol.* **73**, 46–54 (2012).

4. CDER. Application number 21829. Clinical Pharmacology and Biopharmaceutics review(s). (2006).

5. Ito, S. *et al.* Relationship between the urinary excretion mechanisms of drugs and their physicochemical properties. *J. Pharm. Sci.* **102**, 3294–3301 (2013).

6. Irvine, J. D. *et al.* MDCK (Madin − Darby Canine Kidney) Cells: A Tool for Membrane Permeability Screening. *J. Pharm. Sci.* **88**, 28–33 (1999).

7. Chan, M. T. V., Anderson, P. J., Chan, J. C. N., Lau, G. S. N. & Critchley, J. A. J. H. Single-dose pharmacokinetics of paracetamol and its conjugates in Chinese non-insulin-dependent diabetic patients with renal impairment. *Eur. J. Clin. Pharmacol.* **52**, 285–288 (1997).

8. Wootton, R. *et al.* Comparison of the pharmacokinetics of lamotrigine in patients with chronic renal failure and healthy volunteers. *Br. J. Clin. Pharmacol.* **43**, 23–27 (1997).

9. Scotcher, D., Jones, C., Rostami-Hodjegan, A. & Galetin, A. Novel minimal physiologically-based model for the prediction of passive tubular reabsorption and renal excretion clearance. *Eur. J. Pharm. Sci.* **94**, 59–71 (2016).

10. Eriksson, U. G. *et al.* Influence of severe renal impairment on the pharmacokinetics and pharmacodynamics of oral ximelagatran and subcutaneous melagatran. *Clin. Pharmacokinet.* **42**, 743–753 (2003).

11. Zhang, F., Xue, J., Shao, J. & Jia, L. Compilation of 222 drugs' plasma protein binding data and guidance for study designs. *Drug Discov. Today* **17**, 475–485 (2012).

12. Liu, W., Okochi, H., Benet, L. Z. & Zhai, S. Di Sotalol permeability in cultured-cell, rat intestine, and PAMPA system. *Pharm. Res.* **29**, 1768–1774 (2012).

13. Blair, A. D., Burgess, E. D., Maxwell, B. M. & Cutler, R. E. Sotalol kinetics in renal insufficiency. *Clin. Pharmacol. Ther.* **29**, 457–463 (1981).

14. Blum, R. A. *et al.* Pharmacokinetics of gabapentin in subjects with various degrees of renal function. *Clin. Pharmacol. Ther.* **56**, 154–159 (1994).

15. Misaka, S. *et al.* Green tea ingestion greatly reduces plasma concentrations of nadolol in healthy subjects. *Clin. Pharmacol. Ther.* **95**, 432–438 (2014).

16. Herrera, J., Vukovich, R. & Griffith, D. Elimination of nadolol by patients with renal impairment. *Br. J. Clin. Pharmacol.* **7**, 227S-231S (1979).

17. K. Gupta, S., Kantesaria, B. & Glue, P. Exploring the influence of renal dysfunction on the pharmaco-kinetics of ribavirin after oral and intravenous dosing. *Drug Discov. Ther.* **8**, 89–95 (2014).

18. Varma, M. V. *et al.* PH-dependent solubility and permeability criteria for provisional biopharmaceutics classification (BCS and BDDCS) in early drug discovery. *Mol. Pharm.* **9**, 1199–1212 (2012).

19. Houin, G. *et al.* The effects of chronic renal insufficiency on the pharmacokinetics of doxycycline in man. *Br. J. Clin. Pharmacol.* **16**, 245–252 (1983).

20. Frydman, A. M. *et al.* Pharmacokinetics of pefloxacin after repeated intravenous and oral administration (400 mg bid) in young healthy volunteers. *J. Antimicrob. Chemother.* **17 Suppl B**, 65–79 (1986).

21. Montay, G., Jacquot, C., Bariety, J. & Cunci, R. Pharmacokinetics of pefloxacin in renal insufficiency. *Eur. J.*

Clin. Pharmacol. **29**, 345–349 (1985).

22. Frasca, D. *et al.* Metronidazole and hydroxymetronidazole central nervous system distribution: 2. Cerebrospinal fluid concentration measurements in patients with external ventricular drain. *Antimicrob. Agents Chemother.* **58**, 1024–1027 (2014).

23. Houghton, G., Dennis, M. & Gabriel, R. Pharmacokinetics of metronidazole in patients with varying degrees of renal failure. *Br. J. Clin. Pharmacol.* **19**, 203–209 (1985).

24. Barza, M., Brown, R. B., Shanks, C., Gamble, C. & Weinstein, L. Relation between lipophilicity and pharmacological behavior of minocycline, doxycycline, tetracycline, and oxytetracycline in dogs. *Antimicrob.Agents Chemother.* **8**, 713–720 (1975).

25. Avdeef, A. *Absorption and Drug Development*. (John Wiley & Sons, Inc., Hoboken, NJ, USA, 2012).doi:10.1002/9781118286067

26. Welling, P. G., Shaw, W. R., Uman, S. J., Tse, F. L. & Craig, W. A. Pharmacokinetics of minocycline in renal failure. *Antimicrob.Agents Chemother.* **8**, 532–537 (1975).

27. Kirch, W., Ohnhaus, E. E., Dylewicz, P., Pabst, J. & Storstein, L. Bioavailability and elimination of digitoxin in patients with hepatorenal insufficiency. *Am. Heart J.* **111**, 325–329 (1986).

28. Ferry, N. *et al.* Influence of renal insufficiency on the pharmacokinetics of cicletanine and its effects on the urinary excretion of electrolytes and prostanoids. *Br. J. Clin. Pharmacol.* **25**, 359–366 (1988).

29. CDER. Application number 022535. Clinical Pharmacology and Biopharmaceutics review(s). (2014).

30. Naruhashi, K., Tamai, I., Sai, Y., Suzuki, N. & Tsuji, A. Secretory transport of p-aminohippuric acid across intestinal epithelial cells in Caco-2 cells and isolated intestinal tissue. *Journalof Phamrcy and Phamacology* **53**, 73–81 (2001).

31. Prescott, L. F., Freestone, S. & McAuslane, J. A. The concentration-dependent disposition of intravenous p-aminohippurate in subjects with normal and impaired renal function. *Br. J. Clin. Pharmacol.* **35**, 20–9 (1993).

32. Bengtsson, U., Cederbom, G., Falkheden, T. & Jagenburg, R. Clearances of inulin and para-aminohippurate before and after urography using high dosage of contrast medium in patients with renal insufficiency. *Scand. J. Urol. Nephrol.* **2**, 173–176 (1968).

33. FDA Memantine (Namenda): US prescribing information. 1–21 (2010).at <http://www.accessdata.fda.gov/drugsatfda_docs/label/2010/022525s000lbl.pdf>

34. Müller, F. *et al.* Contribution of MATE1 to Renal Secretion of the NMDA Receptor Antagonist Memantine. *Mol. Pharm.* **14**, 1–8 (2017).

35. Periclou, A., Ventura, D., Rao, N. & Abramowitz, W. Pharmacokinetic study of memantine in healthy and renally impaired subjects. *Clin. Pharmacol. Ther.* **79**, 134–143 (2006).